Slope stability under rapid drawdown conditions

E. Alonso & N. Pinyol
Universitat Politècnica de Catalunya, Barcelona

ABSTRACT: The rapid drawdown condition arises when submerged slopes experience rapid reduction of the external water level. Classical analysis procedures are grouped in two classes: the "stress-based" undrained approach, recommended for impervious materials and the flow approach, which is specified for rigid pervious materials (typically a granular soil).

Field conditions often depart significantly from these simplified cases and involve materials of different permeability and compressibility arranged in a complex geometry. The drawdown problem is presented in the paper as a fully coupled flow-deformation problem for saturated/unsaturated conditions. Some fundamental concepts are first discussed in a qualitative manner and, later, explored in more detail through the analysis of two embankment dams. In Shira earthdam pore pressures were recorded at different points inside the embankment as a consequence of a controlled drawdown. Predictions of four calculation procedures (instantaneous drawdown, pure flow, coupled flow-elastic and coupled flow-elastoplastic, all of them for saturated/unsaturated conditions) are compared with measured pressure records. Only the coupled analysis provides a consistent and reasonable solution. The case of a large landslide, immediate to a reservoir, reactivated by a condition of rapid drawdown is also described in the paper.

1 INTRODUCTION

The drawdown condition is a classical scenario in slope stability, which arises when totally or partially submerged slopes experience a reduction of the external water level. Rapid drawdown conditions have been extensively analyzed in the field of dam engineering because reservoir water levels fluctuate widely due to operational reasons. Drawdown rates of 0.1 m/day are common. Drawdown rates of 0.5 m/day are quite significant. One meter/day and higher rates are rather exceptional. However, reverse pumping storage schemes may lead to such fast water level changes in reservoir levels.

Sherard *et al*. (1963) in their book on earth and earth-rock dams describe several upstream slope failures attributed to rapid drawdown conditions. Interestingly, in most of the reported failures the drawdown did not reach the maximum water depth but approximately half of it (from maximum reservoir elevation to approximately mid-dam level). Drawdown rates in those cases were not exceptional at all (10 to 15 cm/day). A Report on Deterioration of Dams and Reservoirs (ICOLD, 1980) reviews causes of deterioration and failures of embankment dams. Thirty-three cases of upstream slips were collected and a third of them were attributed to an excessively rapid drawdown of the reservoir. A significant case was San Luis dam, in California (ICOLD, 1980). San Luis dam is one of the largest earthfill dams in the world (100 m high; 5500 m long; 70 million m^3 of compacted embankment). An upstream slide developed in 1981 after 14 years of successful operation of the dam because of a drawdown, which was more intense than all the previous ones. In this case, the average drawdown rate was around 0.3 m/day and the change in reservoir level reached 55 m. Lawrence Von Thun (1985) described this case. The stability of riverbanks under drawdown conditions is also of concern and Desai (1971, 1972, 1977) in a series of papers describe experimental and theoretical studies performed at the Waterways Experiment Station to investigate the stability conditions of the Mississippi earth banks.

Consider, in qualitative terms, the nature of the drawdown problem in connection with Figure 1.

The position of the water level MO (height H) provides the initial conditions of the slope CBO. Pore water pressures in the slope are positive below a zero pressure line ($p_w = 0$). Above this line, pore water pressures are negative and suction is defined as $s = - p_w$. A drawdown of intensity H_D takes the

free water to a new level M' N' O' during a time interval t_{DD}. This change in level implies:

- A change in total stress conditions against the slope. Initial hydrostatic stresses (OAB against the slope surface; M N B C against the horizontal lower surface) change to O'A'B and M'N'BC. The stress difference is plotted in Figure 1b. The slope OB is subjected to a stress relaxation of constant intensity ($\Delta\sigma = H_D \gamma_w$) in the lower part (BO') and a linearly varying stress distribution in its upper part (O'O). The bottom horizontal surface CB experiences a uniform decrease of stress of intensity, $H_D \gamma_w$.
- A change in hydraulic boundary conditions. In its new state, water pressures against the slope are given by the hydrostatic distribution O'A'B on the slope face and by the uniform water pressure value $p_w = (H - H_D) \gamma_w$ on the horizontal lower surface.

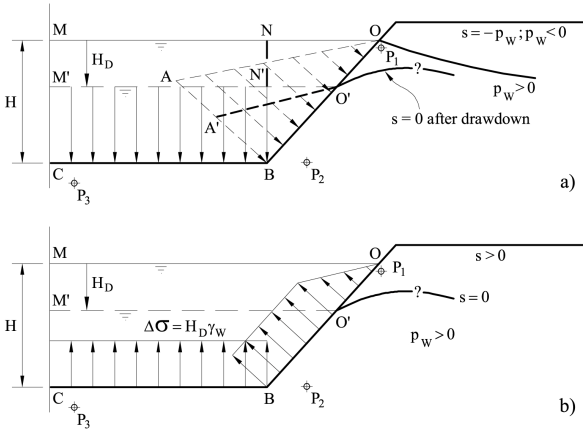

Figure 1. The drawdown scenario: (a) Hydrostatic stresses acting against the exposed slope surface. (b) Change in applied stresses on the exposed boundaries induced by a drawdown H_D

The change in hydrostatic pressures against the slope surface induces also a change in total stress inside the slope. This stress change will produce, in general, a change in pore pressure. The sign and intensity of these pore pressure depend on the constitutive (stress-strain) behaviour of the soil skeleton. An elastic soil skeleton will result in a change of pore pressure equal to the change in mean (octahedral) stress. If dilatancy (of positive or negative sign) is present, due to shear effects, additional pore water pressures will be generated. The resulting pore pressures will not be in equilibrium with the new boundary conditions and a transient regime will develop. If soil permeability is high pore pressures will dissipate fast, perhaps concurrently with the modification of boundary conditions. This situation will constitute a "drained" reaction of the slope. In fact, velocity of drawdown and permeability should be considered jointly in order to decide if the slope reacts in a drained or undrained manner. In practice, however, drawdown rates vary between narrow limits and the soil permeability becomes the dominant parameter.

Skempton (1954) and Henkel (1960) provided expressions for the development of pore pressures (p_w) under undrained conditions before modern constitutive equations were born. The B coefficient of the well known Henkel expression is given by:

$$B = \left(\frac{1}{1 + n \dfrac{K'_{skel}}{K_w}} \right) \tag{1}$$

where n is the soil porosity; K'_{skel}, the bulk modulus of the soil skeleton, and K_w, the bulk modulus of water. K_w is close to K_w = 2100 MPa and, therefore, in practically all cases involving compacted materials in dam engineering, $K'_{skel} << K_w$ and $B = 1$. Even for an exceptionally stiff soil material or soft rock ($K'_{skel} \cong K_w$) the value of B is close to 1. This is a well-known result but it is often read, in connection with drawdown analysis, that in cases of rigid materials the (stress) uncoupled flow analysis is sufficiently accurate, implying that no stress-related changes in pore pressures are generated. It is clear that this is never the case in practice.

Two classes of procedures have been developed to analyze drawdown. The first class highlights the effect of changing boundary stresses in order to calculate the pore water pressures immediately after a (sudden) drawdown. The second class of procedures uses pure Darcy-type flow, and they are said to be valid for rigid (!) and pervious materials. It is also common, at present, to find flow-based stress uncoupled analysis in practical applications and, therefore, a distinction of the results likely to be found in case of stress coupled or uncoupled (pure flow) analysis is useful for discussion.

Figure 2 shows in qualitative terms the expected evolution of pore pressures in a representative point (P_2) of the slope, plotted in Figure 1, during a drawdown which takes place in a time interval, t_{DD}.

Points such as P1, in the upper part of the slope will experience a small change in stresses. During drawdown they will likely become unsaturated. Away from the upstream slope (point P_3 in Fig. 1) stress effects associated with the slope geometry disappear and pore pressures will follow the changing levels of the reservoir. However, the behaviour of point P_2, close to the slope toe, is strongly controlled by the stress state induced by drawdown. The resulting pore pressures during the drawdown process will be affected by the rate of water level lowering, the "map" of initial pore pressures, (which, in turn, depend on the stress field), and by the source terms associated with the volume change experienced by the soil skeleton – controlled by soil stiffness- and any possible change in saturation conditions. Figure 2

indicates that the uncoupled analysis (which makes the assumption of rigid soil) leads, in the case of an impervious soil, to the prediction of the highest pore pressures inside the slope. If the soil is definitely pervious no difference between coupled or uncoupled hypothesis will be found. Most cases in practice will remain in an intermediate zone, which will require a coupled analysis for a reasonable pore pressure prediction.

A reference to the usual expression of time to reach a given degree of consolidation, U, in one-dimensional consolidation problems, provides a clue on the effect of soil stiffness:

$$t = \frac{L^2 T(U)}{k \quad E_m} \gamma_w \tag{2}$$

where L is a reference length associated with the geometry of the consolidation domain; T is the time factor; k, the soil permeability, E_m, the confined stiffness modulus, and γ_w, the water specific unit weight.

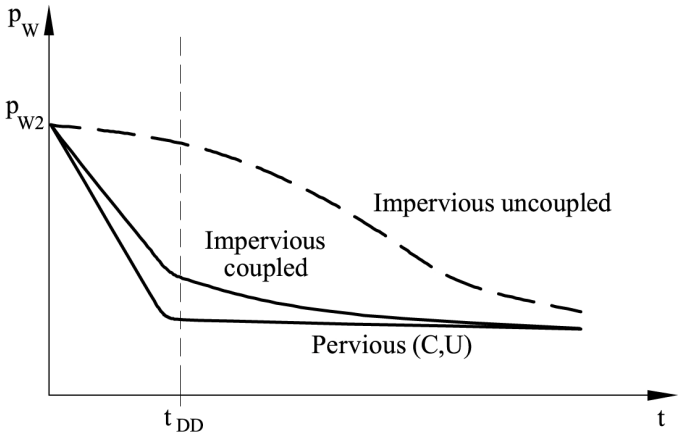

Figure 2. Change in pore water pressures in Point P_2 for coupled or uncoupled analysis and pervious or impervious fill.

Soft materials (E_m low) will react with high consolidation times, all the remaining factors being maintained. Figure 3b indicates this effect. Permeability and stiffness control the rate of pore pressure dissipation in this case, in the manner indicated. However, if more advanced soil models are introduced, the simple trends given in Figure 3 may change.

The changing boundary condition and the soil permeability essentially control the transient behaviour of the uncoupled model (Fig. 3a). Note that a comparison of Figures 3a and 3b does not provide clear indication of the relative position of the pressure dissipation curves. Therefore, it is difficult to define "a priori" the degree of conservatism associated with either one of the two approaches. Of course, it is expected that the fully coupled approach should provide answers close to actual field conditions.

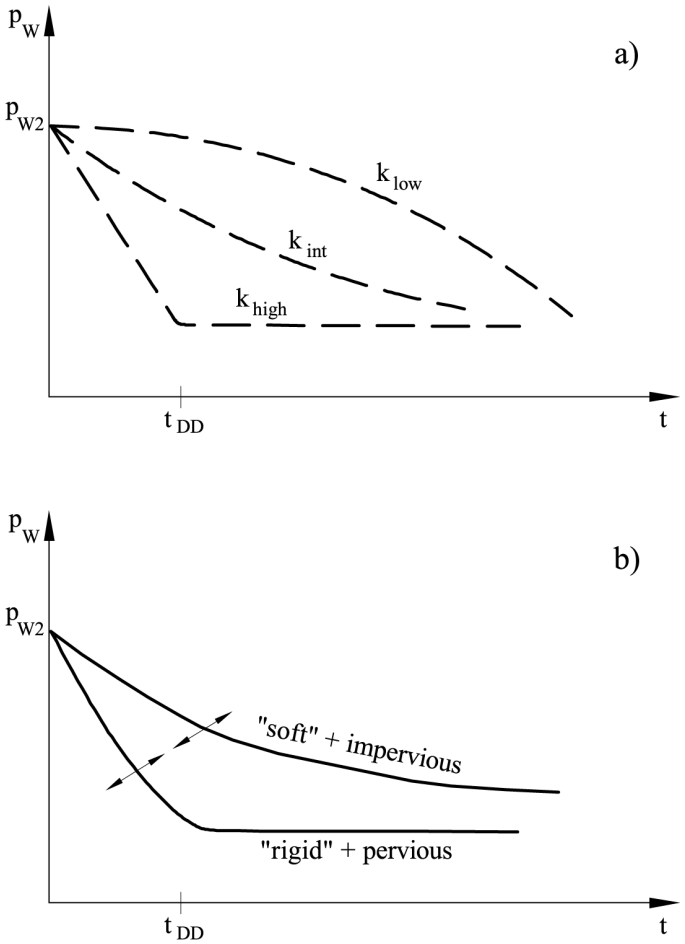

Figure 3. Change in pore water pressures in point P_2 for (a) uncoupled analysis or (b) coupled analysis.

This paper describes modern procedures to deal with the drawdown problem in a general case of saturated/unsaturated conditions. After a brief account of previous developments the analysis of a simple slope will be presented. Then some applications will be developed. They refer to two embankment dams and to a recent case of a large landslide on the bank of a reservoir, triggered by rapid drawdown conditions. All the calculations reported here were performed with CODE_BRIGHT, a FE program for THM analysis developed at the Department of Geotechnical Engineering of UPC (DIT-UPC, 2002). Unsaturated soil behaviour follows the elastoplastic model BBM (Alonso et al, 1990)

2 BRIEF HISTORICAL PERSPECTIVE

The literature describes two approaches to predict the pore water pressure regime after drawdown: the undrained analysis and the flow methods.

The aim of the undrained approach is the determination of pore water pressures immediately after drawdown in impervious soils. Skempton (1954) derived first his well-known expression in terms of soil parameters A and B (or $\overline{B}$). In his wording:

The "overall" coefficient $\overline{B}$ is a useful parameter, especially in stability calculations involving rapid drawdown, and it can be measured directly in the laboratory for the relevant values of stress-changes in a particular problem.

Only the change in major principal stress is required to use Skempton's $\overline{B}$ parameter. Bishop (1954) followed this recommendation and assumed that the major principal stress in any point within the slope is the vertical stress. He proposed also that the change in weight, statically computed in a column of soil and water above a reference point, would provide $\Delta\sigma_1$. Finally he suggested $\overline{B}$ = 1 as an appropriate value in practice. Bishop's approach has been criticized because it may lead to unacceptable large negative pore water pressures under the dam (Baker *et al*., 1993).

Morgenstern (1963) accepted Bishop's proposal based on a correspondence between Bishop's method and pore pressures measured in two dams subjected to rapid drawdown (Alcova and Glen Shira dams). It is not clear that results of Glen Shira dam follow Bishop's recommendation, however. Morgenstern published plots providing safety factors after drawdown in terms of drawdown ratio (H_D/H in Fig. 1) for different values of slope angle, effective cohesion and effective friction. The dam geometry was simple: a homogeneous triangular dam on an impervious base. Much later, Lane and Griffiths (2000) solved a similar case in terms of geometry, but failure conditions were calculated by means of a (c', φ') reduction procedure built into a finite element program, which uses a Mohr-Coulomb failure criterion. They do not solve any flow equation in their program and it is not clear how they could derive the pore water pressures induced by total stress unloading.

Lowe & Karafiath (1980) and Baker *et al*. (1993) performed undrained analyses to calculate the safety factors of slopes under rapid drawdown conditions. The analysis is applicable to relatively impervious soils and it does not require a determination of pore pressures after drawdown (which is required for a drained analysis of the type performed by Morgenstern). Instead, the idea is to find the distribution of undrained strengths for the particular stress state just before drawdown. However, the emphasis in this paper lies on the determination of pore pressures after drawdown so that general effective stress analysis could be performed.

Flow methods probably started with the contribution of Casagrande (1937), who developed a procedure to find the time required to reach a certain "proportion of drainage" of the upstream shell of dams having an impervious clay core. By assuming a straight saturation line, he was able to derive some analytical expressions. Later Reinius (1954) demonstrated the use of flow nets to solve slow drawdown problems. This contribution was based on earlier work published in Sweden. The key idea is that:

[...] the flow net at slow drawdown is determined by dividing the time in intervals and assuming the reservoir water level to be stationary and equal to the average value during the interval.

He also computed, based on the Swedish friction circle method of analysis, safety factors during drawdown and plotted them in terms of a coefficient (k/nv), which integrates the soil permeability (k), the porosity (n) and the rate of drawdown, v. He also explained, in the following terms, the pore water pressure generation due to rapid drawdown:

When the reservoir is lowered rapidly the total stresses decrease. If the soil does not contain air bubbles and the water content remains unchanged, the effective stresses in the soil also remains unchanged provided that the compressibility of the water is neglected. Hence the neutral stresses must decrease.

A similar statement may be found in Terzaghi and Peck (1948). Examples of flow net construction for drawdown conditions may be found in Cedergren (1967).

Finite difference approximations and, later, finite element techniques were used in the 60's and 70's to calculate the flow regime under drawdown conditions. The major problem was to predict the location of the phreatic surface during drawdown. When Dupuit-type of assumptions -horizontal flow- is made (Brahma & Harr, 1962; Stephenson 1978) the location of the zero-pressure surface comes automatically from the analysis. When solving the Laplace equation by finite elements (Desai, 1972, 1977), some re-meshing procedures were devised. An additional example of a determination of the free surface is given in Cividini & Gioda (1984).

In parallel, the liquid water flow equation for unsaturated porous media was being solved by means of finite difference or finite element approximations (Rubin, 1968; Richards & Chan, 1969; Freeze, 1971; Cooley, 1971; Neumann, 1973; Akai *et al*., 1979; Hromadka & Guymon, 1980, among others). These developments made it obsolete the involved numerical techniques required to approximate the free surface through the saturated flow equation. Berilgen (2007) published recently a contribution to the drawdown problem. The author used two commercial programs for transient/flow and deformation analysis respectively. He reported a sensitivity analysis involving simple slope geometry. Safety factors are calculated by a (c', φ') reduction method built into the mechanical finite element program. The author emphasized that the undrained rapid drawdown case and the fully drained case (high

permeability) are rough approximations for other intermediate situations likely to be found in practice.

Pauls *et al*. (1999) reports a case history. A stress-uncoupled finite element program was used to analyze the pore pressure evolution in a river bank as a result of a flooding situation. Consistently, predicted pore pressures remained well above the measured piezometric data. One possible explanation, not given in the original paper, is the uncoupled nature of the computational code used. In fact, no riverbank failures were observed in this case despite the calculated safety factors, lower than one.

2.1 *Drawdown in a single slope*

Consider the case sketched in Figure 1. A fully submerged simple slope will experience a drawdown condition when the water level acting against the slope surface is lowered. The actual geometry of the slope analyzed is given in Figure 4. The figure indicates the position of three singular points used in the discussion: A point at mid slope (P_A), a point at the slope toe (P_B) and a point away from the slope (P_C) which is representative of "bottom of the sea" conditions. Three auxiliary vertical profiles will assist in the analysis of results.

An elastic constitutive law will characterize the soil. Concerning the hydraulic description, Figure 5 indicates the water retention curve and the relative permeability law adopted in calculations. The retention curve (Fig. 5) has been defined by means of a Van Genuchten model and the relative permeability varies with the degree of saturation following a cubic law ($k_{rel} = k_{sat} S_r^3$). A constant saturated permeability k_{sat} = 10^{-10} m/s was also used in all calculations

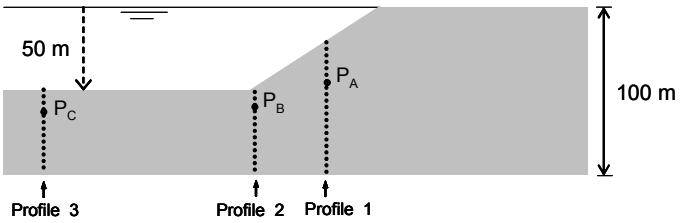

Figure 4. Geometry of the slope. Labels indicate the position of three singular points mentioned in the discussion.

The initial state of pore pressure will be hydrostatic (Fig. 6). Consider first the case of a total and rapid drawdown. If the analysis is performed uncoupled, no change in pore pressures inside the slope will be calculated immediately after drawdown. This is the case plotted in Figure 7, which was obtained with program Code_Bright when only the flow calculation was activated. Note that Figures 6 and 7 provide essentially the same distribution of water pressures.

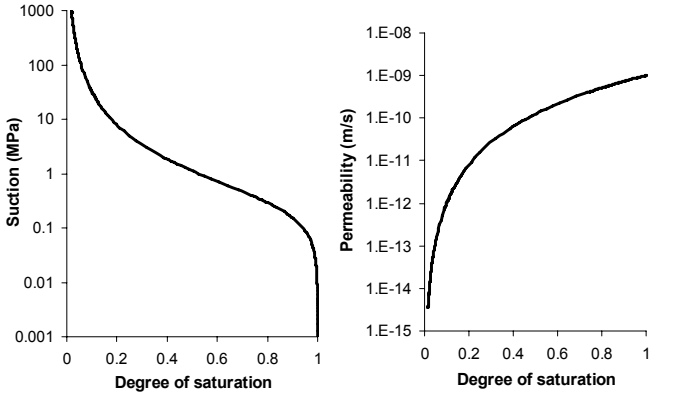

Figure 5. Retention curve and relative permeability function for the analysis of a simple slope.

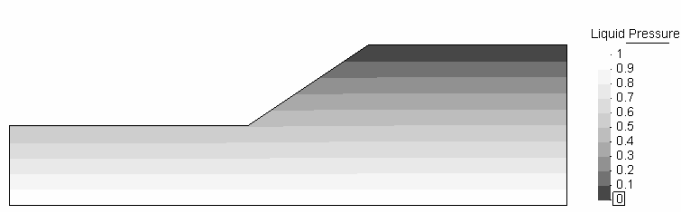

Figure 6. Initial pore water pressure distribution before drawdown.

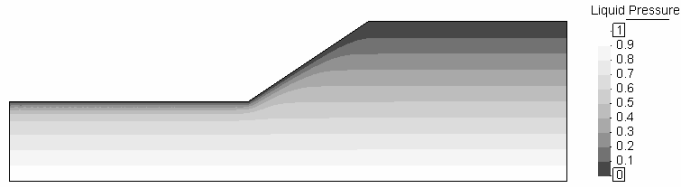

Figure 7. Pore water pressure distribution after immediate drawdown in an uncoupled analysis.

A realistic condition concerning the drawdown rate (v = 0.5 m/day) will be imposed in the cases presented here. During drawdown boundary conditions of the upstream slope will follow a "seepage face condition": the boundary is assumed impervious unless the calculated water pressure at the boundary becomes positive. In this case water flows out of the slope following a "spring" type of condition. Three elastic moduli spanning the range 100-10000 MPa are considered. They cover the majority of situations in practice for compacted upstream shells of dams (especially for small to medium shear strains). The saturated permeability considered is a low value in order to highlight the differences between coupled and uncoupled analysis. Of course, these differences decrease as the soil becomes more pervious.

Consider first the case of the "bottom of the sea" conditions (Fig. 8). All the coupled analyses lead essentially to the same response. This is because variations in the instantaneous response are erased by the simultaneous dissipation of pressures. For the stiffer materials considered (E = 1000, 10000 MPa), water pressures remain slightly above the values found in

common cases soils. However, the pure flow analysis is far from the correct answer.

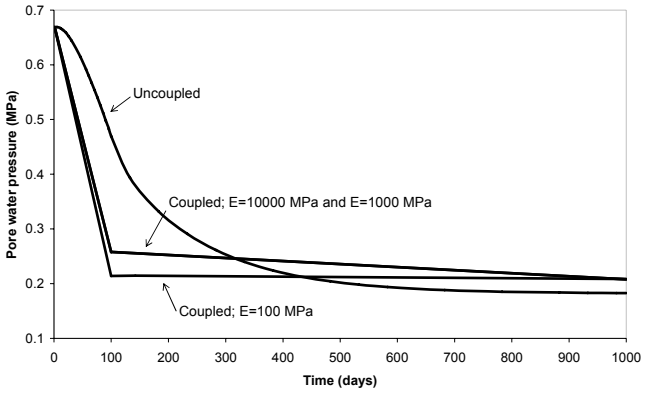

Figure 8. Pore water pressure evolution after progressive drawdown in point P_C (see Fig. 4).

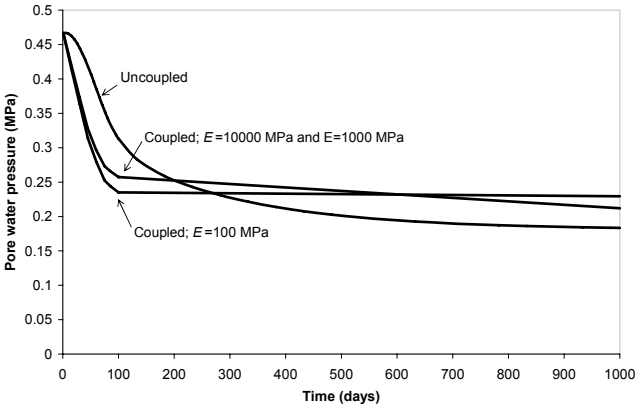

Figure 9. Pore water pressure evolution after progressive drawdown in the point P_A (see Fig. 4)

Similar results were obtained for the three reference points. Only the case of the mid slope point is plotted in Figure 9.

It may be argued that the pure flow analysis is a conservative approach if viewed in terms of slope safety against failure. However, this is a result which depends on the particular case considered and cannot be generalized. It is also interesting to realize that the unrealistic uncoupled analysis leads to a lower pore pressure prediction in the long term. This is a result of the implicit assumption of infinite skeleton stiffness of the uncoupled calculation, which leads to faster dissipation rates than the coupled approach.

3 DRAWDOWN ANALYSIS OF SAN SALVADOR DAM

Some relevant results of the drawdown analysis performed on San Salvador earthdam, which has recently been designed, are now discussed. Parameters for the analysis are given in Table 1. They were determined from tests performed at the design stage of the dam.

Figure 10 shows a comparison of calculated pore water pressures alter drawdown for the coupled and uncoupled cases. The analyzed drawdown corresponds to the design specifications: reservoir level decreases 24 m in 60 days. Calculated pore pressures in the upstream shell, core and foundation under the hypothesis of uncoupled analysis are significantly higher than in the coupled case. This is clear also in Figures 11-13 which provide the evolution of pore water pressures in three representative points of the dam: two in the foundation and a third one in the shell, close to the core. Figure 11 indicates that non-coupled analyses are unable to reproduce an elementary result: pore pressures under the bottom of the reservoir should follow, in an essentially instantaneous manner, the variations of reservoir water level. The uncoupled analysis results in pore pressures higher than the level in the reservoir.

A similar result is observed in a profile directly affected by the dam (below the upstream toe; see Fig. 14). Three cases are represented: initial profile, profile immediately after drawdown and long term. In the correct coupled analysis pore pressures after drawdown are higher than the hydrostatic long term values. This is due to the presence of the dam and the particular stress distribution associated with changes in total stresses against the boundary of the dam and the foundation soil. Pure flow analysis results in abnormally high pore water pressures.

Table 1. Parameters for the drawdown analysis of San Salvador dam.

Parameter	Symbol	Unit	Foundation	Upstream shell	Core
Young Modulus	E	MPa	150	100	30
Coefficient of volumetric compressibility	m_w	MPa^{-1}	$4.95x10^{-3}$	$7.42 \cdot 10^{-3}$	$2.47 \cdot 10^{-2}$
Saturated permeability	k_{sat}	m/s	$1 \cdot 10^{-9}$	$1.8 \cdot 10^{-9}$	$2.81 \cdot 10^{-10}$
Retention curve (Van Genuchten)	P_0	MPa	0.5	0.05	0.5
	λ	-	0.24	0.4	0.24
	S_{rmax}	-	1	1	1
	S_{rmin}	-	0.01	0.075	0.01

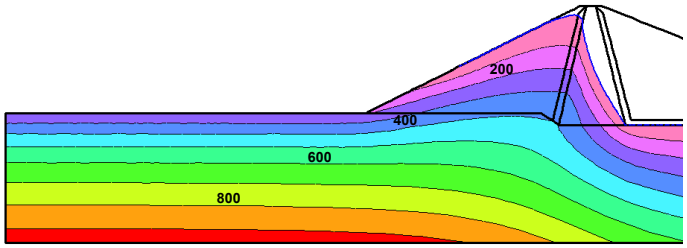

(a)

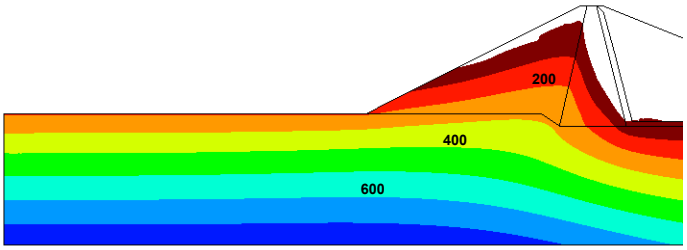

(b)

Figure 10. Pore water pressure contours. The represented interval is 100 kPa. (a) Uncoupled analysis. (b) Flow-deformation coupled analysis.

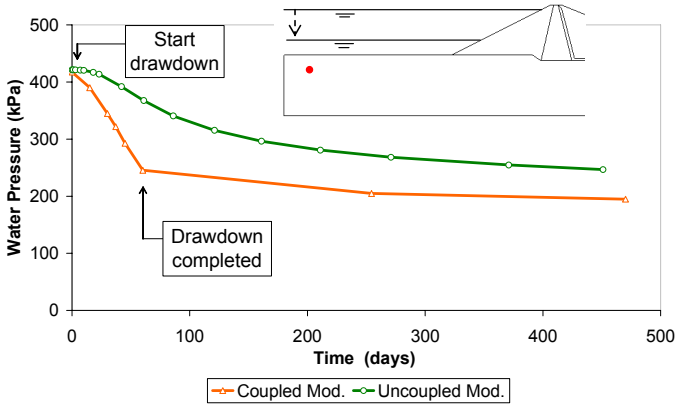

Figure 11. San Salvador dam. Evolution of pore pressures in a point distant from the dam toe, during drawdown and subsequent times.

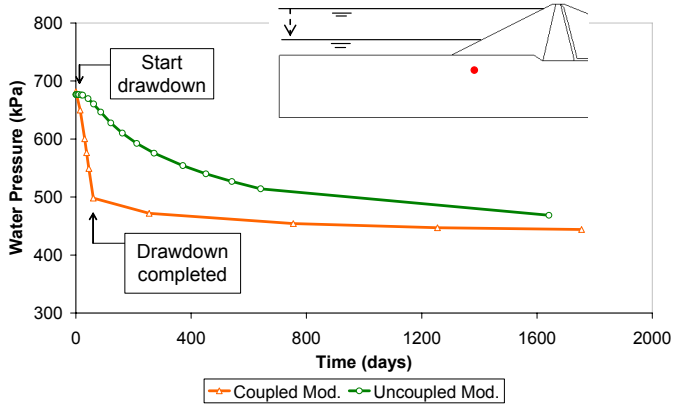

Figure 12. San Salvador dam. Evolution of pore pressures in a point within the foundation, Ander the upstream shell during drawdown and subsequent times

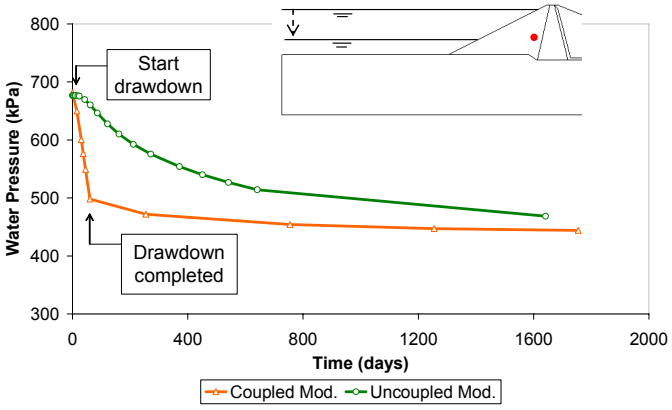

Figure 13. San Salvador dam. Evolution of pore pressures in a point within the upstream shell, close to the core, during drawdown and subsequent times

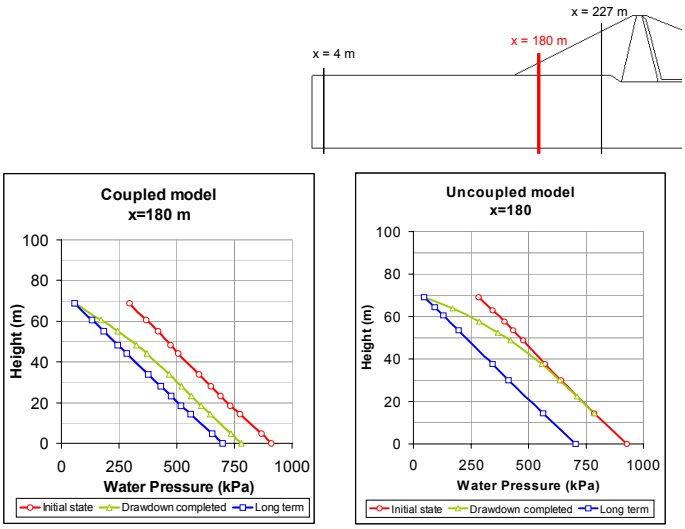

Figure 14. San Salvador dam. Vertical profiles at the toe of the dam. Comparison of coupled and uncoupled analyses.

4 GLEN SHIRA DAM CASE HISTORY

Glen Shira Lower Dam is part of a pumping storage scheme in Northern Scotland. The reservoir was expected to experience fast drawdown rates and this situation prompted the field experience reported by Paton and Semple (1961). Probably this is one of the best-documented case histories concerning the effect of drawdown on earth dams. The maximum cross section of the dam is presented in Figure 15. The 16 m high embankment has a centered thin reinforced concrete wall. The homogeneous embankment is made of compacted moraine soil. A rockfill shell covers the upstream slope of the compacted moraine to increase stability. Published grain size distributions of the moraine soil indicate a well-graded material having a maximum size of 15 cm. Plasticity is not reported for this soil. It was apparently compacted wet of optimum at an average water content w = 15%. The attained average dry density was 19.8 kN/m^3, which is a relatively high value for a granular mixture. A friction angle ϕ' = 36º is reported.

For the rockfill a porosity of n = 0.4, a dry density of 16.7 kN/ m^3 and a friction angle ϕ' = 45º are mentioned in the paper.

Table 2. Hydraulic parameters used for the analysis of Shira dam.

Definition of parameter	Symbol	Units	Type of soil	
			Moraine	Rockfill
Saturated permeability	k_{sat}	m/s	1.6. 10^{-8}	1.0. 10^{-4}
Relative permeability	k_{rel}	-	$k_{sat}\,(S_w)^3$	$k_{sat}\,(S_w)^3$
Van Genuchten parameter describing air entry value	p_0	MPa	0.05	0.01
Van Genuchten parameter describing mid slope of retention curve	λ	-	0.2	0.4

Five porous stone piezometer disks, previously calibrated against mercury columns, were located in the places shown in Figure 15. They were connected to Bourdon gauges through thin polyethylene tubing. The authors conclude in their paper that the possibility of instrumental error are "of minor order and can be neglected".

No significant pore water pressures were recorded during construction. Positive pore pressures were measured only after reservoir filling

A total water level drawdown of 9.1 meters in four days was applied to Glen Shira dam. This maximum drawdown was imposed in four stages of rapid (7.2 m/day) water lowering followed by short periods of constant water level. Details of changing water level in the reservoir and the measured pore water pressures are indicated in the set of figures prepared to analyze this case.

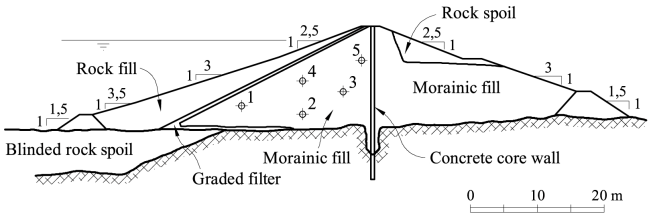

Figure 15. Maximum cross section of Shira Dam. The position of piezometers 1 to 5 is indicated

The following hypotheses, ordered in the sense of increasing complexity, were made to perform calculations:

1. A pure flow analysis for saturated/unsaturated conditions that follows the changing hydraulic boundary conditions actually applied to the upstream slope. Table 2 provides the hydraulic parameters used in calculations. These parameters are common to the remaining analyses described below.

2. An instantaneous drawdown of the maximum intensity, followed by pore water pressure dissipation. This is a coupled analysis, which attempts to reproduce the classical hypothesis behind the undrained methods, briefly described in the introduction of the paper. The procedure does not correspond strictly to Bishop's method because in the analyses reported here the correct change in total stresses is actually applied. The soil was simulated as an elastic material (propert. are given in Table 3).

3. A coupled analysis (saturated/unsaturated), following the applied upstream changes in hydrostatic pore pressures. The soil is considered elastic (properties are given in Table 3).

4. A coupled analysis (saturated/unsaturated) following the applied upstream changes in hydrostatic pore pressures. The soil is considered elasto-plastic following the BBM model, Alonso et al (1990), (properties are given in Table 3). The elastic parameters of this model are taken from the previous elastic model.

The case of Shira dam is especially interesting because the permeability of the compacted moraine fill (around 10^{-8} m/s; see below) is an intermediate value between impervious clay and a free draining material. One may wonder to what extent the classical hypothesis for drawdown analysis (undrained or pure flow) approximates the actual behaviour. This aspect will be discussed later.

The following ideas have guided the selection of parameters. The elastic (unloading-reloading) moduli of compacted moraine and rockfill are typical of a stiff soil. In fact, well graded granular mixtures become rather stiff when compacted. The virgin compressibility, $\lambda(0)-\kappa$, is approximately one order of magnitude higher than the elastic compressibility. Parameters r and β controls the shape of the yield LC curve of BBM. The moraine soil is assumed to gain limited stiffness as suction increases (parameter r). Also, the increase in stiffness with suction is fast for relatively low values of suction and remains fairly constant thereafter (parameter β). The slope of the critical state strength line reflects the friction angles provided in the paper. Zero cohesion is assumed throughout the analysis, irrespective of suction (parameter k_s). A small reference stress (p_c) is assumed. Associated yield conditions were assumed in both materials (parameter α=1). Rockfill properties were assumed to be similar to the compacted moraine, except for the higher friction angle.

Table 3. Parameters for the mechanical models used for the analysis of Shira dam

Definition of parameter	Symbol	Units	Type of soil	
			Moraine	Rockfill
I. ELASTIC BEHAVIOUR				
Elastic modulus	E	MPa	100	100
Poisson's ratio	ν	-	0.3	0.3
II. PLASTIC BEHAVIOUR				
Virgin compressibility for saturated conditions	$\lambda(0)-\kappa$	-	0.020	0.020
Parameter that establishes the minimum value of the compressibility coefficient for high values of suction	r	-	0.8	0.8
Parameter that controls the rate of increase in stiffness with suction	β	MPa^{-1}	6.5	6.5
Reference stress	p^c	MPa	0.01	0.01
Slope of critical state strength line	M	-	1.4 (35º)	1.85 (45º)
Parameter that controls the increase in cohesion with suction	k_s	-	0	0
Parameter that defines the non-associativeness of plastic potential	α	-	1	1
III. INITIAL STATE FOR DAM MODEL				
Initial suction	s_0	MPa	0.01	0.01
Initial yield mean net stress	p_o^*	MPa	0.01	0.01

The dam was built in a single step. A more detailed representation of dam construction plays a minor role in the analysis of drawdown. The following "as compacted" initial suction and saturated yield stress were imposed: $s_0 = 0.01MPa$ and $p_0^* = 0.01MPa$. Given the low value of p_0^* which reflects the isotropic yield state after compaction, dam conditions at the end of construction correspond to a normally consolidated state. The dam was then impounded until steady state conditions were reached. The presence of the impervious concrete membrane results in a simple initial state: all points upstream of the concrete wall maintain hydrostatic water pressure conditions. This initial state correspond to day 5 in the plots presented later.

The information given in the original paper provided data to approximate hydraulic parameters. Two saturated values of permeability are mentioned for compacted specimens in the laboratory ($1.6\cdot10^{-8}$ m/s, when compacted at optimum water content and $1.6\cdot10^{-7}$ m/s when compacted wet of optimum). However, the dry densities reached in the field (19.8 kN/m^3) are higher than the optimum laboratory B.S. compaction (19.3 kN/m^3) and this leads to a reduction in permeability. A saturated permeability value k_{sat} = $1.6\cdot10^{-8}$ m/s was therefore selected for field conditions.

Water retention properties for the moraine were derived following a simplified procedure, which makes use of the grain size distribution. Since the moraine soil is a granular material, capillary effects will dominate the water retention properties. On the other hand, pore size distributions may be approximated if grain size distributions are known. An example is given, for beach sand, in Alonso and Romero (2003). The idea is that the pore size distribution follows the shape of the grain size distribution. However, the pore diameter is a fraction of the equivalent grain size. In the sand reported by Alonso and Romero (2003) this fraction is approximately 0.25. It is probably lower in a well-graded

material although this ratio was accepted to derive the pore size distribution from the known average value of the grading curve for the moraine soil. The next step is to use Laplace equation to derive the suction emptying a given pore size. This leads immediately to the water retention curve. The Van Genuchten expression fitted to the derived water retention curve corresponds to parameters (see also Table 2): p_0 = 0.05 MPa and $\lambda = 0.2$. The rockfill retention curve was approximated with a significantly lower air entry value (lower p_0) and an increased facility to desaturate (higher λ) when suction is applied. Finally, a cubic law, in terms of the degree of saturation, defined the relative permeability.

Figures 16 to 20 illustrate the performance of the different methods of analysis (1. to 4.) listed above. Consider first the hypothesis of instantaneous drawdown (9.5 m of water level drawdown, instantaneously). The calculated pressure drop is indicated in the figures by means of a vertical bar. A (coupled) dissipation process is then calculated and the progressive decay in pore pressures is also plotted. If compared with the actual pore pressures measured at the end of the real drawdown period, the hypothesis of instantaneous drawdown leads obviously to an extremely pessimistic and unrealistic situation. (The end point of the instantaneous drawdown at t = 9 days is to be compared with the pore pressure recorded at the end of the drawdown period at t = 12.4 days).

Table 4. Shira dam. Instantaneous drawdown. Comparison of coupled and simplified (Bishop) analysis

Piezometer	Initial pressure (horizontal water table) (kPa)	Calculated instantaneous pressure drop (Code_Bright) (kPa)	Bishop hypothesis $\Delta u = B\ \Delta\sigma_V$ B =1 (kPa)
1	96	42	42
2	106	22	12
3	67	10	1
4	56	17	12
5	23	6	0

It is also interesting to compare the results of the fully coupled analysis of the instantaneous drawdown with the approximated method of analysis suggested by Skempton/Bishop. Table 4 shows the comparison. The change in vertical stress ($\Delta\sigma_v$) has two contributions: the change in free water elevation above a given point and the decrease in total specific weight of the rockfill material covering the moraine shell. An effective saturated porosity of 0.3, after drainage, was assumed to calculate the drop in total specific weight. Bishop hypothesis leads systematically to a higher pore pressure drop than the more accurate analysis. This is specially the case for the piezometers located deep inside the fill. Discrepancies are due to the simplified stress distribution assumed in the approximate method.

Consider now the opposite calculation method: a pure flow analysis. In this case, Figures 16 to 20 indicate that the predicted pore pressures are the lowest ones if compared with the remaining methods of analysis. Calculated water pressures follow closely the history of reservoir levels. The "damping" effect associated with soil compressibility is absent. When the water level is increased, at the end of the drawdown test, the pure flow analysis indicates, against the observed behaviour, a fast recovery of pore pressures within the embankment.

Coupled analyses are closer to actual measurements. This is true in absolute terms but also in the trends observed when boundary conditions (changes in reservoir level) are modified.

Construction of Shira Dam leaves most of the embankment under normally consolidated conditions. This is a consequence of the low initial yield stress, p_0, adopted in the analysis. p_0 is related to the energy of compaction, but a detailed discussion of this topic is outside the limits of this paper. Granular materials, and certainly rockfill, tend to yield under low stresses after compaction. Therefore, the accumulation of layers over a given point will induce plastic straining. The stress paths in points relatively away from the slope surfaces follow K_0 – type of conditions. Figure 21 indicates the stress path of points located in the position of Piezometers 1 and 3. Plotted in the figure are also the yield surfaces at the end of construction. The maximum size of the yield surface corresponds to these construction stages. Once the dam is completed, reservoir impoundment leads to a reversal of the stress path, which enters into the elastic zone. Drawdown leads to a new sharp reversal in the stress path and the increase in deviatoric stresses. However, the end of the drawdown path remains inside the elastic locus in the two cases represented in Figure 21.

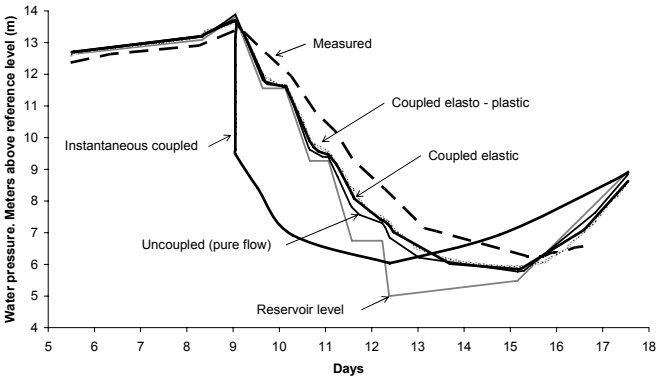

Figure 16. Comparison of measured pore pressures in Piezometer 1 and different calculation procedures.

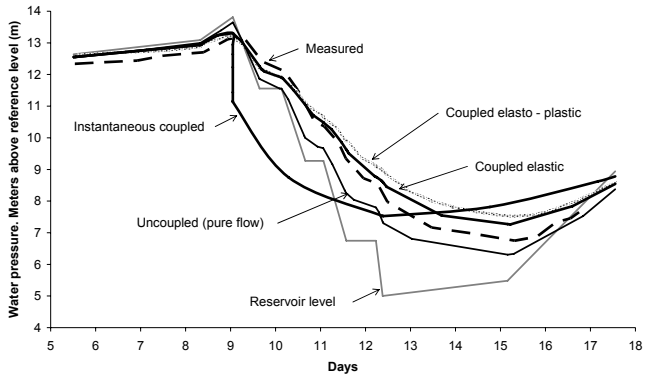

Figure 17. Comparison of measured pore pressures in Piezometer 2 and different calculation procedures.

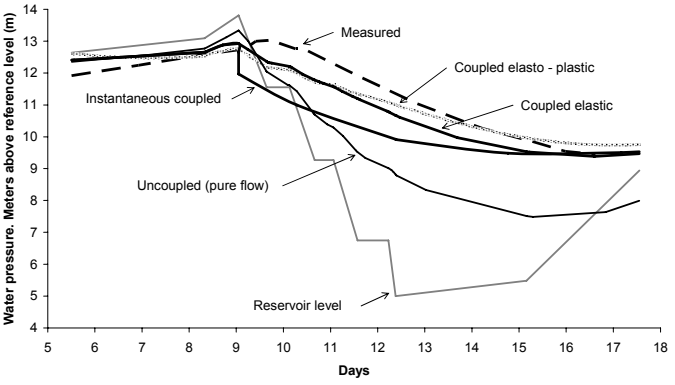

Figure 18. Comparison of measured pore pressures in Piezometer 3 and different calculation procedures.

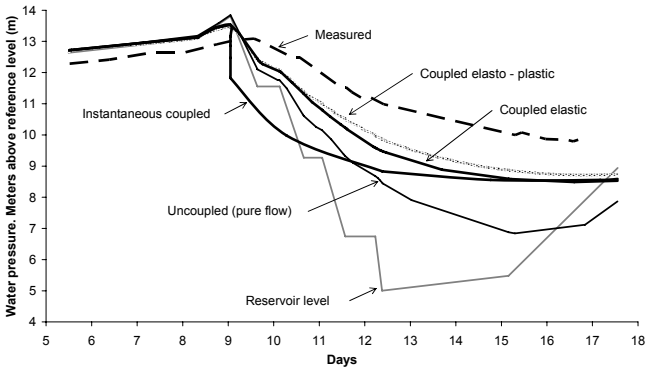

Figure 19. Comparison of measured pore pressures in Piezometer 4 and different calculation procedures

The possibility of inducing additional plastic straining during drawdown depends on the geometry of the dam cross section and on the constitutive behaviour of the materials involved. Shira dam has a stable geometry because of the low upstream slope (3 to 1) and shear stresses inside the dam are relatively small. In addition, the granular shell material has a high friction angle (35º). However, under different circumstances, plastic straining may develop during drawdown, and, in this case, pore pressures will probably increase because the yield point, located in the "wet" (compression) side of the yield locus (see Fig. 21) implies that additional local sources of local excess pore pressures are available for dissipation. Note also the differences in calculated stress paths for piezometers 1 and 3 during drawdown. Piezometer 3 is located deep inside the embankment, at a high elevation and therefore pore pressure changes are small: the effective mean stress remains constant and the stress path moves vertically upwards. However, the change in deviatoric stresses is also small and the final stress point is far from reaching critical state conditions. Piezometer 3, on the contrary, is close to the upstream shell, at a lower elevation. Changes in pore pressure and deviatoric stress are large in this position and the stress path moves approximately parallel to the initial construction path and approaches yielding conditions in compression.

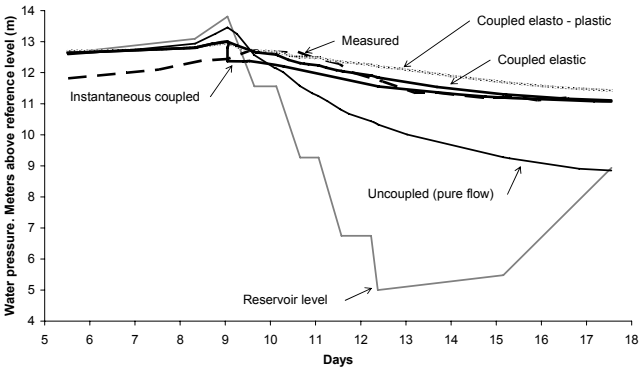

Figure 20. Comparison of measured pore pressures in Piezometer 5 and different calculation procedures.

There is, however, an additional effect, which leads to a different drawdown behaviour when comparing elastic and elastoplastic modelling approaches. If permeability is made dependent on void ratio, the construction of the dam will lead to lower values of permeability (distributed in a heterogeneous manner). If the compacted dam material yields during construction, plastic volumetric compaction will add to the elastic strains. In addition, collapse phenomena upon impounding will reduce further the porosity. These effects have been also explored in the case of Shira dam. Permeability was made dependent on void ratio, *e*, following a Kozeny type of relationship (permeability depends on $e^3/(1+e)$). The calculated records of pore pressure evolution during drawdown are also shown in Figures 16 to 20. The reduction in permeability, if compared with the coupled elastic case, leads to a systematic increase in pore pressures. The agreement with measurements is now better in some piezometers (1, 3 and 4).

(a)

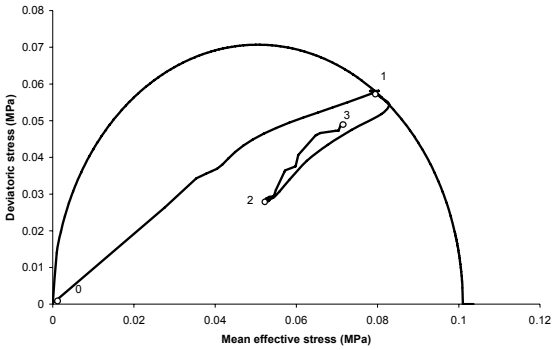

(b)

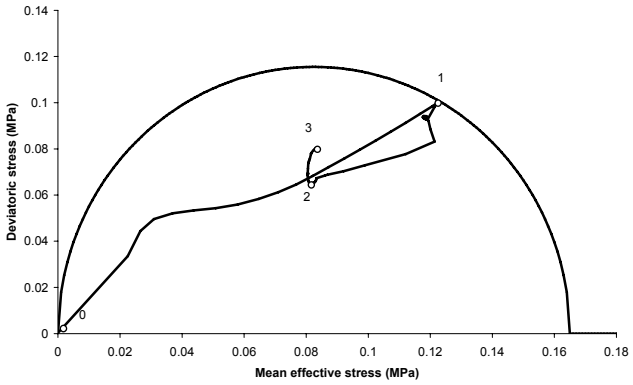

(b)

Figure 21. Stress path in a (q,p') triaxial stress space of points located in the position of piezometers 1 and 3 during construction, impoundment and drawdown. 0-1: Construction; 1-2: Impoundment; 2-3: Drawdown. Also plotted are the yield surfaces at the end of construction

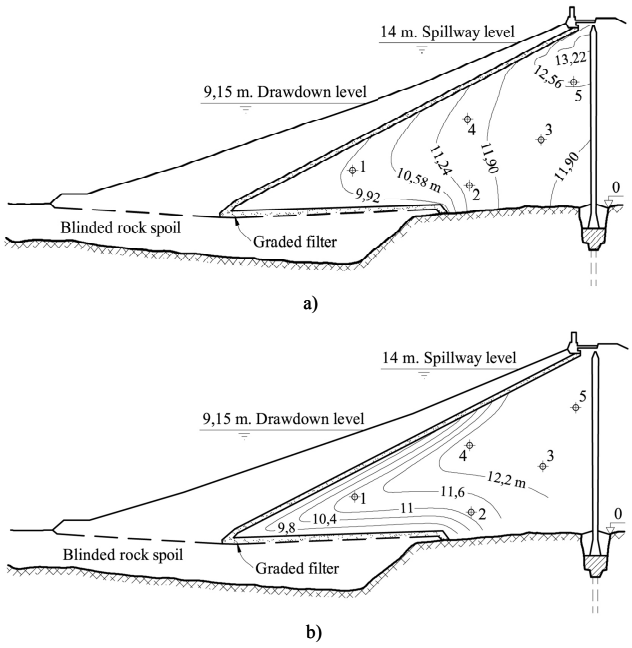

Figure 22. Distribution of pore pressures inside the shell for a drawdown 14 to 9.15 m. a) Computed results (coupled analysis); b) Interpolated values plotted by Paton and Semple (1961)

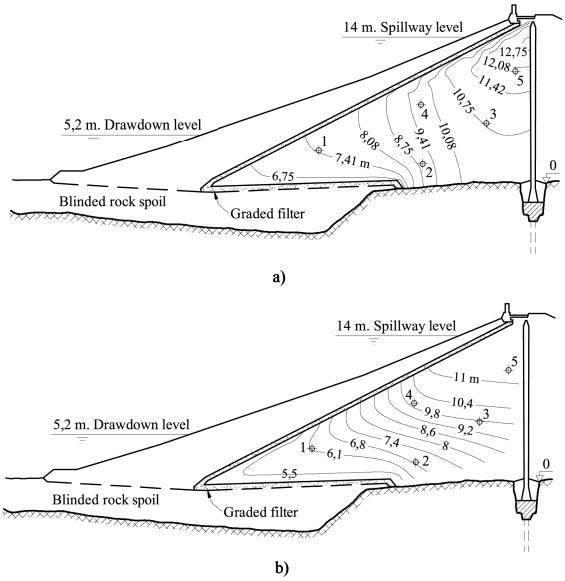

Figure 23. Distribution of pore pressures inside the shell for a drawdown 14 to 9.15 m. a) Computed results (coupled analysis); b) Interpolated values plotted by Paton and Semple (1961)

Paton and Semple (1961) plotted also contours of piezometric head during drawdown. Two examples are given in Figures 22b and 23b. They correspond to drawdown drops of 4.85 and 8.8 m. The reservoir level reaches 9.15 and 5.2 m respectively (with respect to the zero reference level which in this paper is placed at the dam base: point 0 in Figures 22 and 23). The authors used the data recorded on the five piezometers to interpolate the curves shown in the figure. They made the hypothesis of a zero water pressure at the shell-rockfill interphase. The computed distribution of heads inside the dam shell, for the same amount of drawdown, is also plotted in Figures 22a and 23a (coupled elastic analysis). The agreement is quite acceptable, although some discrepancies exist, which, in part could be attributed to the limited accuracy of the interpolation made.

The conclusion, for the particular embankment material of Shira dam and its overall geometry and design, is that the classical methods of analysis are far from explaining the recorded behaviour. The "instantaneous" or undrained method is conservative, but very unrealistic. A fully coupled analysis of the instantaneous drawdown results in higher pressure drops than the classical Bishop proposal. At the opposite extreme, the pure flow analysis leads to a systematic and unsafe underestimation of fill pressures during drawdown. Coupled analysis captures well the actual measurements. In the case of Shira dam, plastification during drawdown was probably nonexistent, and the simpler elastic approach provides a good approximation to recorded pore water pressures. However, the full elastoplastic simulation offers a better understanding of the phenomena taking place during construction and impounding. This is shown in the stress paths calculated, in the occurrence of yielding during construction, and in the ef-

fect of permeability reduction on the drawdown response.

5 CANELLES LANDSLIDE

5.1 *General setting*

The left margin of Canelles reservoir (Huesca, Aragón, Spain) is a sequence of subhorizontal thick units of Cretacic and Paleogene origin. Lower hard limestones are covered by levels of the Garum facies which includes claystones and limestones. The clay levels exhibit high plasticity (w_L=54-57%), PI=27-31%) and are known to be involved in slope stability problems at regional scale. The reservoir serves several purposes: irrigation, electric generation and fluvial control. Rapid drawdown conditions are associated to irrigation demands in dry climatic periods.

In the summer of 2006 a long continuous tensile crack, more than one kilometer in length, parallel to the reservoir water line created some alarm. Investigations performed immediately afterward allowed to identify a large landslide whose volume was estimated in $30 \cdot 10^6$ m^3 (Fig. 24).

The crack was located at the foot of continuous scarp 4 to 5 m high which was identified as a limiting boundary of an ancient slide (Figre 25). It was concluded that some phenomena reactivated suddenly the slide on the summer of 2006.

Figure 24. Aerial view of Canelles reservoir and landslide contour indicated with the yellow line. (Approximate length of yellow line: 1.8 km)

Most probably the slide was reactivated by a rapid drawdown condition on the neighboring reservoir. Figure 26 shows a multiyear record of water levels in the reservoir. The maximum historic drawdown rate was close to 0.5 m/day and these velocities were measured on the month of July/August 2006.

Figure 25. Detail of a tension crack at the foot of an ancient scarp. The motion of the slide (on the left) looks essentially translational.

Deep borings with a continuous recovery of cores were performed. In some of them vibrating wire piezometers and inclinometers were installed. However the landslide remained essentially at rest after the first alarming crack developed and the inclinometers could not provide a clear indication on the position and shape of the sliding surface.

This large landslide raises two major concerns:

- The possible development of a catastrophic failure which would invade the water of the reservoir.
- The restriction which should be imposed on the reservoir operation to maintain in adequate level of safety.

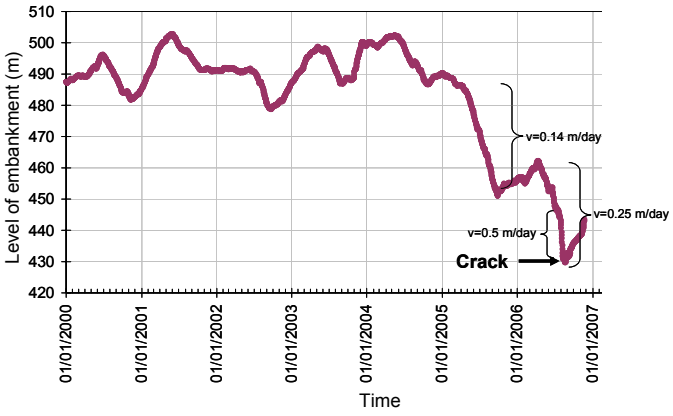

Figure 26. Reservoir level history.

Figure 27. Striated shear surfaces. Boring SI-1-1 at a depth of 58.75 m.

As a first and fundamental information, it was necessary to establish with certainty the shape of the rupture surface(s). The answer to this crucial question was provided by a detailed examination and interpretation of recovered cores. It was found that striated shearing planes were systematically located within the Garum clay facies (Fig. 27). A representative cross section of the slide is given in Figure 28. It shows a profile located approximately on the central axis of the slide. The profile shows the sequence of main strata and the position of boreholes. Also some levels of the water in the reservoir are indicated as a general reference.

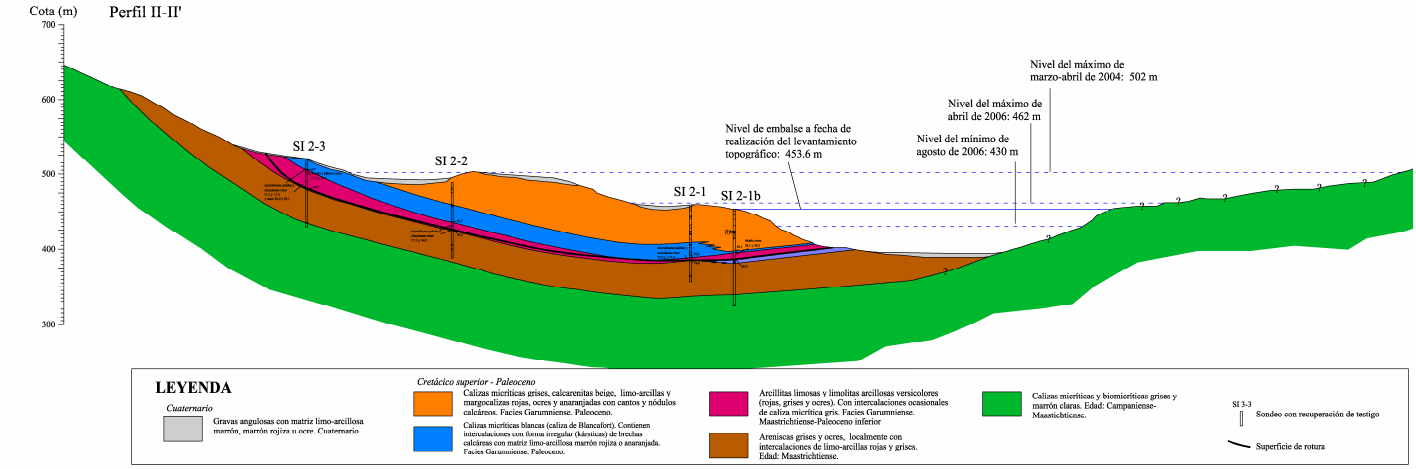

Figure 28. Representative cross-section of the landslide

Accordingly, the frictional angle available in the natural sliding surface can be slightly lower than the value measured in the laboratory. On the other hand, back analysis of similar cases of reactivated landslides indicate that the available residual frictional angle of striated natural sliding surface is lower than the value obtained in ring shear tests on remoulded samples. For these two reasons, in the backanalysis of this case, presented below, the residual frictional angle considered has been taken equal to 10º, 2º lower than the value obtained in the laboratory.

5.2 *Relevant material properties*

Remoulded samples from the Garum clay strata, where sliding surfaces is located, were tested in laboratory. A permeability test at constant hydraulic load provided a low value of permeability equal to $4 \cdot 10^{-10}$ m/s. Ring shear test were also carried out to determine the residual frictional angle of the material. Figure 29 shows the obtained results. The maximum applied vertical stress was 200 kPa. It is significantly lower than the vertical stress acting on the sliding surface which can reach values close to 1800 kPa in the deepest parts. In general, secant frictional angle decreases with the normal stress applied.

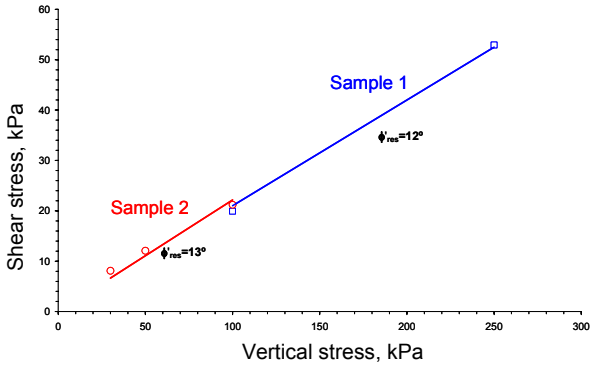

Figure 29. Ring shear test results

5.3 *Numerical Analysis*

5.3.1 *Back analysis*

A central section of the slide has been chosen for the numerical analysis of the Canelles slide during the

drawdown (Fig.30). A hydro-mechanical coupled analysis was carried out with the finite element program Code_Bright in order to calculate the pore pressure distribution after the drawdown. Stability analysis considering the obtained pore pressure distribution after drawdown was performed with the commercial program Slope (GEO/SLOPE International Ltd. Calgary, Alberta, Canada).

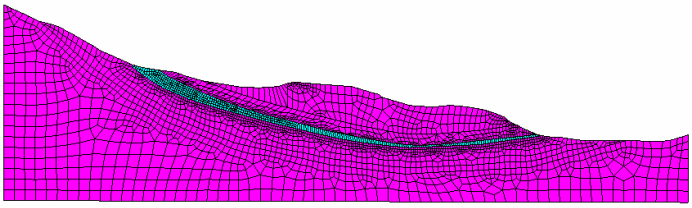

Figure 30. Cross section analyzed

Figure 30 shows the finite element mesh. Materials have been defined by means of a linear elastic law characterized by Young modulus and Poissons' ratio. The analysis of Glen Shira Dam presented above indicates that the effect of including an elastoplastic law in the modelling drawdown is limited, specially for relatively stiff materials and moderate slope, which is the case. For simplicity and because of the lack of detailed data, the claystones and limestones above and below of the clay strata have been simulated by a unique material characterized by the elastic parameters indicated in Table 5. Parameters of clay level are also indicated in the Table. The expected lower stiffnes of the Garum clay level is reflected in the table.

Table 5. Mechanical and hydraulic parameters for Canelles Landslide

Parameter and unit	Clay strata	Limestone/claystones
Young modulus (MPa)	500	2500
Poisson's ratio	0.3	0.3
Saturated permeability (m/s)	$4 \cdot 10^{-10}$	10^{-6}
Van Genuchten Parameters:		
λ	0.33	0.33
P_0 (MPa)	0.3	0.01
Sr_{max}	1	1
Sr_{min}	0	0

The obtained value of saturated permeability of the clay sample in the laboratory ($4 \cdot 10^{-10}$ m/s) has been introduced in the calculation. The permeability value of the rock mas, above and below the clay strata, has been estimated equal to 10^{-6} m/s (a few orders of magnitude higher). Retention curves have been defined according to Van Genuchten model. The chosen values for parameters are indicated also in Table 5. The main difference between the more pervious limestone and marl strata and the clay formation lies in the air entry value.

Reservoir level history has been simulated. Figure 26 shows the reservoir level data measured during seven years, before the formation of the crack. Only the last four years, before the reactivation, have been modelled. The reservoir level remained between 480 and 500 m for a long period (from the beginning of 2000 to the summer of 2004) (Fig. 26). According with this, a stationary hydraulic condition defined by a reservoir level at elevation 480 m has been defined as initial condition (Fig. 31). It corresponds to the October 2002. After that, the reservoir level history during the following four years has been modelled according to the actual recorded reservoir elevation.

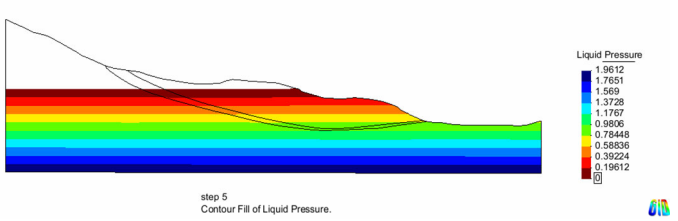

Figure 31. Pore water pressure distribution. Initial condition (only positive values have been indicated).

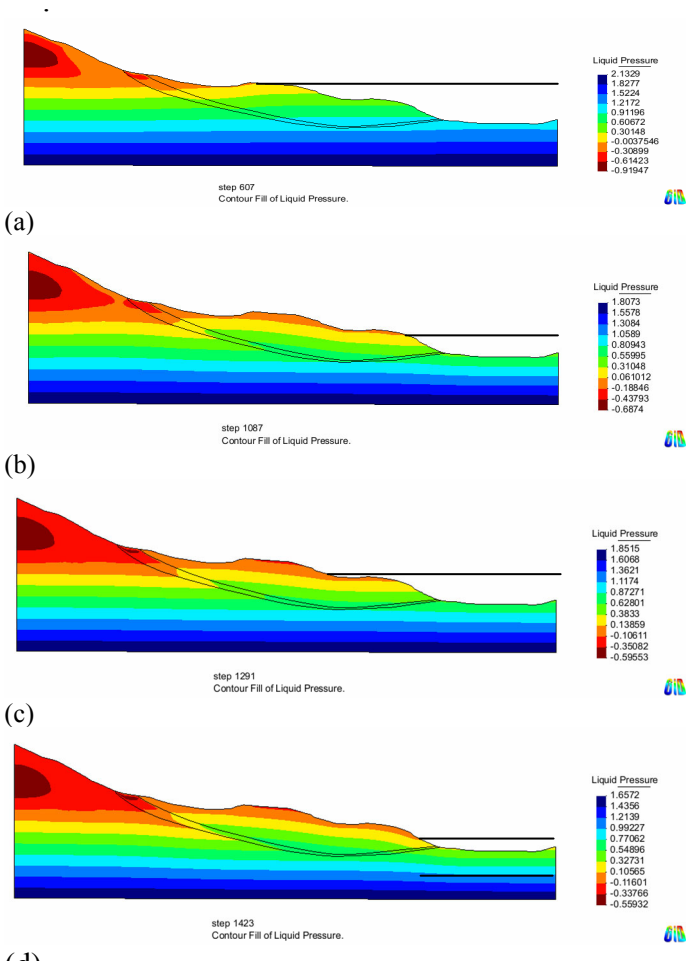

Figure 32. Calculated pore water pressure distribution at (a) April 2004; (b) September 2005; (c) April 2006; and (d) August 2006, when crack was first observed (see Fig. 26).

Rainfall has also been considered in the analysis performed. In this case a constant average value has been calculated from a meteorological station located near the reservoir. A constant flow equivalent to 400 l/m^2 per year has been imposed as a boundary condition on the surface of the landslide above the reservoir level.

Figure 32 shows the water pore pressure distribution at different stages. The horizontal black line indicates the position of the reservoir level. The effect of the imposed flow simulating the rain can be observed in the upper part of the slopeIt is interesting to realize the important effect of the fine impervious clay strata on the pore pressure distribution in the slope.

Stability analysis after the drawdown has been calculated taking into account the pore pressure distribution indicated in Figure 32d. No effect of suction has been introduced. Therefore, only positive pore pressures have been considered in the stability analysis. However, the length of sliding surface affected by negative pressures is small compared with its overall length. The slide surface has been predefined according to field observations. Figure 33 shows the section used in the stability analysis and the position of the specified slide surface. The slide surface only crosses the clay strata. Therefore, only the strength properties of this material are relevant in this analysis. The strength response has been defined by a Mohr Coulomb law with cohesion equal to zero (residual conditions) and frictional angle equal to 10º, as discussed before.

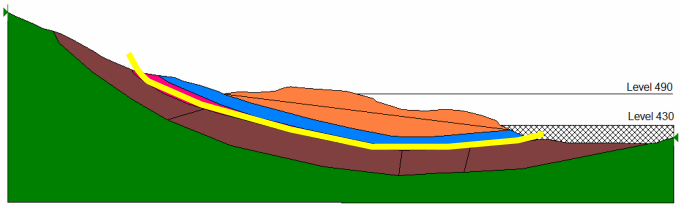

Figure 33. Cross section for stability analysis. Specified slide surface is indicated in yellow.

According to the laboratory tests the value of the density of the clay for calculation is 18 kN/m^3. The density of the unstable rock has been estimated equal to 20 kN/m^3.

These parameters yield a safety factor of 0.98, following the Morgenstern-Price method. This is in good agreement with field observations.

6 CONCLUSIONS

Pore water pressures in an initially submerged slope and later subjected to drawdown depend on several soil parameters and “external” conditions: soil permeability (saturated and unsaturated), soil water retention properties, mechanical soil constitutive behaviour, rate of water level lowering and boundary conditions. The paper stresses that a proper consideration of these aspects is only possible if a fully coupled flow – mechanical analysis, valid for saturated and unsaturated conditions is employed. A review of the literature on the subject reveals that the published procedures are plagued with numerous assumptions, which prevent often its use in real problems and make it difficult to judge on the degree of conservatism -if any- introduced.

Leaving apart for the moment the issue of the transition from saturated to unsaturated conditions which takes place during drawdown, there are two fundamental mechanisms controlling the resulting pore water pressure: the change in pore pressure induced by boundary changes in stress and the new flow regime generated. Both of them require a coupled analysis for a proper interpretation and consistency of results. In particular, pure flow models are unable to consider the initial changes in pore pressure associated with stress unloading. The intensity of pore pressure changes induced by a stress modification is controlled by the soil mechanical constitutive equation. In a simplified situation, under elastic hypothesis for the soil skeleton, the pore pressure depends on the ratio of soil bulk stiffness and water compression modulus. In most situations, this ratio is small and the influence of soil effective stiffness is negligible. This implies a maximum response of the saturated material to stress changes. Without this coupling, the initial pore pressures do not change during fast unloading.

Permeability and soil stiffness controls coupled flow. The uncoupled analysis implicitly assumes a rigid soil and therefore it leads to a maximum dissipation rate. Both effects (the initial change in pore pressure and the subsequent dissipation) should be jointly considered for a better understanding of the evolution of pore pressures. In addition, the rate of change of boundary conditions is key information to interpret the results. No simple rules can be given to estimate the pore pressures in the slope. This is even more certain if due consideration is given to the unsaturated flow regime.

A well documented case history (Shira dam) was analyzed to provide further insight into the drawdown problem. The case is very interesting because the soil involved (a compacted moraine) has an intermediate permeability between impervious clays and free draining granular materials. It should be added that materials with this intermediate permeability are very common in engineering. Therefore, the two classical procedures to analyze drawdown effects (undrained analysis for clays and pure flow for granular materials) will meet difficulties. In fact, these two methods proved to be quite unrealistic when compared with actual records of pore water pressures in different points of the dam. In particular, the pure flow (uncoupled) analysis leads to faster dissipation of pore pressures and this is an unsafe result in terms of stability calculations. The

fully coupled analysis (elastic or elastoplastic) provides consistent results.

In a final chapter of the paper the recent case of a large landslide, immediate to Canelles reservoir, triggered by rapid drawdown conditions, has been illustrated. The analysis performed is the first step towards establish safe operational practices in the reservoir in order to avoid the landslide reactivation in the future.

7 REFERENCES

Akai, K., Ohnishi, Y., Murakami T. & Horita, M. 1979. Coupled stress flow analysis in saturated/unsaturated medium by finite element method. *Proc. Third Int. Conf. Num. Meth. Geomech*. 1: 241-249, Aachen.

Alonso, E. E., Gens, A. and Josa, A. 1990. "A constitutive model for partially saturated soil". Géotechnique 40 No. 3, 405-430.

Alonso, E.E. & Romero, E. 2003. Collapse behaviour of sand. *Proceedings of the 2nd Asian Conference on Unsaturated Soils. Osaka*. 325-334.

Baker, R, Rydman, S & Talesnick, M. 1993. Slope stability analysis for undrained loading conditions. *Int. Jnl. Num. and Anal. Methods Geomech*. 17: 14-43.

Brahma, S.P. & Harr, M.E. 1962. Transient development of the free surface in a homogeneous earth dam. *Géotechnique* 12: 283-302.

Casagrande, A. 1937. *Seepage through dams. Contributions to soil mechanics*, 1925-1940. Boston Society of Civil Engineers.

Cividini, A. & Gioda, G. 1984. Approximate F. E. analysis of seepage with a free surface. *International Journal for Numerical and Analytical Methods in Geomechanics* 8 (6): 549-566.

Cedergren, H.R. 1967. *Seepage, drainage and flow nets.* New York.

Cooley, R. L. 1971. A finite difference method for unsteady flor in variable saturated porous media: Application to a single pumping well. *Water Res. Res*. 7 (6): 1607-1625.

Desai, C.S. & Shernan, W.C. 1971. Unconfined transient seepage in sloping banks. *Jnl. of the Soil Mech. and Found. Div*. ASCE, Nº SM2: 357-373.

Desai, C.S. 1972. Seepage analysis of earth banks under drawdown. *Jnl. of the Soil Mech. and Found. Div., ASCE*, Nº SM11: 1143-1162.

Desai, C.S. 1977. Drawdown analysis of slopes by numerical method. *Jnl. of the Soil Mech. and Found. Div., ASCE*, Nº GT7: 667-676.

DIT-UPC (2002) CODE_BRIGHT. A 3-D program for thermo-hydro-mechanical analysis in geological media. USER'S GUIDE. Centro Internacional de Métodos Numéricos en Ingeniería (CIMNE), Barcelona.

Freeze, R. S. 1971. Three dimensional transient saturated-unsaturated flow in a groundwater basin. *Water Res. Res*. 7 (2): 347-366.

ICOLD 1980. *Deterioration of dams and reservoirs. Examples and their analysis*. ICOLD, Paris. Balkema, Rotterdam.

Henkel, D.J. 1960. The shear strength of saturated remoulded clays. *Proc. ASCE Research Conference on Shear Strength of Cohesive Soils* Boulder: 533-554.

Hromadka, T. V. & Guymon, G. L. 1980. Some effects of linearizing the unsaturated soil moisture transfer diffusivity model. *Water Res. Res*. 16 (4), 643-650.

Lane, P.A. & Griffiths, D.V. 2000. Assessment of stability of slopes under drawdown conditions. *Jnl. Geotech. and Geoenv. Engng*. 126(5): 443-450.

Lawrence Von Thun, J. 1985. San Luis Dam upstream slide, *Int. Conf. on Soil Mech. Found. Eng.* 11, 2593– 2598.

Lowe, J. & Karafiath, L. 1980. Effect of anisotropic consolidation on the undrained shear strength of compacted clays. *Proc. Research Conf. on Shear Strength of Cohesive Soils*. Boulder: 237-258.

Morgenstern 1963. Stability charts for earth slopes during rapid drawdown. *Géotechnique* 13(1):121-131.

Neumann, S.P. 1973. Saturated-unsaturated seepage by finite elements. Jnl. Hydraul. Div., ASCE, 99, HY12: 2233-2250.

Pauls, G.J., Karlsauer, E., Christiansen, E.A. & Wigder, R.A. 1999. A transient analysis of slope stability following drawdown after flooding of highly plastic clay. *Can. Geotech. Jnl.* 36: 1151-1171.

Paton, J., & Semple, N.G. 1961. Investigation of the stability of an earth dam subjected to rapid drawdown including details of pore pressure recorded during a controlled drawdown test. *Pore pressure and suction in soils*: 85-90. Butterworths, London.

Reinius, E. 1954. The stability of the slopes of earth dams. *Géotechnique* 5: 181-189.

Richards, B.G. & Chan, C.Y. 1969. Prediction of pore pressures in earthdams. *Proc. 7th Int. Conf. S.M.F.E.*, 2: 355-362. Mexico

Rubin, J. 1968. Theoretical analysis of two-dimensional transient flow of water in unsaturated and partly saturated soils. *Soil Sci. Soc. Am. Proc*. 32 (5): 607-615.

Sherard, J.L., Woodward, R.J. Gizienski, S.F. & Clevenger, W.A. 1963. *Earth and earth-rock dams*. John Wiley and Sons, New York.

Skempton, A.W. 1954. The pore pressure coefficients A and B. *Géotechnique* 4(4), 143-147.

Stephenson, D. 1978. Drawdown in embankments. *Géotechnique* 28(3): 273-280.

Terzaghi, K. & Peck, R.B. 1948. *Soil mechanics in engineering practice.* Wiley, New York.